

Effects of anhydrous AlCl_3 dopant on the structural, optical and electrical properties of PVA–PVP polymer composite films

G Shanmugam^{1*} and V Krishnakumar²

¹Department of Physics, Vel Tech, Chennai, Tamilnadu 600 062, India

²Advanced Materials Laboratory, Department of Physics, Periyar University, Salem, Tamilnadu 636 011, India

Received: 17 June 2016 / Accepted: 22 September 2017 / Published online: 13 December 2017

Abstract: Polymer composite films based on PVA–PVP with AlCl_3 as the dopant at different concentrations were prepared using solution casting technique. XRD patterns reveal the increase in amorphousness of the films with AlCl_3 doping. Optical absorption studies exhibit that the values of optical absorption coefficient, direct and indirect optical band gaps are found to decrease with increase in AlCl_3 concentration. It confirms the charge transfer in complexes between the polymer and the dopant. The dielectric studies show the increase in dielectric constant at low frequency with increasing AlCl_3 concentration and temperature. The ac conductivity and ionic conductivity increase with the AlCl_3 content and the maximum value at room temperature is found to be 6.89×10^{-4} and 8.05×10^{-5} S/cm for higher AlCl_3 doped PVA–PVP film. The estimated ionic conductivity value is three or four orders of magnitude greater than those obtained in the certain representative polymer-salt complexes as reported earlier. Electrical modulus plots confirm the removal of electrode polarization and the low conductivity relaxation time with Al doping. The activation energy estimated from the temperature dependent dc conductivity plot is agreed well with the migration energy calculated from the temperature dependent electric modulus plot.

Keywords: Polymer composite film; Amorphous phase; Optical energy band gap; Dielectric property; Ionic conductivity

PACS Nos.: 77.84.Jd; 72.80.Le

1. Introduction

Electrical conductivity studies on polymer films have been extensively studied due to their potential applications in various electrochemical devices such as sensors, solid state batteries, fuel cells, electrochromic display devices, super capacitors, etc. [1–4]. The low cost and facile preparation of polymer films make them as the promising candidates for wide variety of applications. However, the low ionic conductivity of polymer films at ambient temperature has limited their potential applications. The major efforts in this field have remained concentrated in developing new polymer electrolytes with high ionic conductivity and high mechanical, thermal and electrochemical stability. In recent years, studies on the electrical and optical properties of polymer composites have attracted much attention in

view of their potential applications in electronic and optical devices. The main advantage of the polymer composites is that they are able to dissociate the ion-pairs into free cations and anions. The dissociation of ions leads to overall conductivity enhancement, simplicity of preparation and ease of control of physical properties by compositional change [5–10]. Polymer composites usually contain both crystalline and amorphous phases but conductivity occurs only in the amorphous phase. In order to increase the conductivity at ambient temperature, polymer composites help to reduce the crystalline content and enhance the amorphous content. Also the film formability with desirable mechanical, thermal and electrochemical stability makes polymer composites more attractive than the conventional materials [11, 12].

Among the polymers, poly vinyl alcohol (PVA) is most interesting polymer because of its high dielectric strength and thermal stability, good charge storage capacity and dopant-dependent electrical and optical properties. PVA is

*Corresponding author, E-mail: gvshanmugamphysics@gmail.com

a semi-crystalline polymer which contains both amorphous and crystalline phases at room temperature. Moreover it has a carbon chain backbone with hydroxyl groups attached to methane carbons. These -OH groups can be a source of hydrogen bonding and hence of assistance in the formation of polymer blends [13–15]. For preparing polymer composite with PVA, poly vinyl pyrrolidone (PVP) was chosen as second polymer. PVP is an amorphous polymer and it forms a variety of complexes with various salts, due to the presence of carbonyl group (C=O) in the side chain of PVP, which can permit faster ionic mobility. It also deserves a special attention because of its good environmental stability, easy processability, moderate electrical conductivity and rich physics in ionic transport mechanism [16, 17]. Both PVA and PVP are industrially most important water soluble polymers which are miscible in all proportions and their composites have potential applications in the fabrication of electrochemical devices.

The structural, optical, and electrical properties of polymer composites can be suitably modified by the addition of the migrating ion species depending on their reactivity with the host matrix. Until recently most of the migrating ion species had been only limited to mono- and divalent ions, and some of them have been already brought to the market in many industrial fields [13–17]. In this regard, a target for the next generation is to develop a trivalent ion conducting polymer composites. Among the trivalent cations, Al^{3+} is the most abundant metal ion and the third most abundant element in the earth's crust. This metal ion also involves three electron transfers during the electrochemical charge/discharge reactions, provides competitive storage capacity relative to the single-electron Li metal ion. Al^{3+} ion has consequently long attracted attention because of its high specific energy, low atomic mass and small ionic radius as well as its low cost [18, 19]. Furthermore, the literature survey surprisingly indicated that there is no report on the complete study of ion transport properties of anhydrous aluminium chloride (AlCl_3) doped solid polymer composite films exists. In view of the above factors, for first time we report the PVA–PVP polymer composites doped with the various concentrations of AlCl_3 prepared using solution casting technique. The influence of AlCl_3 dopant on structural, optical and electrical properties of PVA–PVP polymer composite films over a wide range of frequency and temperature has been studied in detail.

2. Materials and methods

We used PVA ($M_w = 14,000$, Kemphasol, India), PVP ($M_w = 40,000$, HiMedia Laboratories Pvt. Ltd, India) and anhydrous AlCl_3 (Nice Chemicals Pvt. Ltd, India) to

prepare PVA–PVP and AlCl_3 doped PVA–PVP polymer composite films. All the chemicals were used as received. PVA and PVP (50:50 wt%) were dissolved in the doubly distilled water with stirring at 80 °C. Required quantity (0, 10 and 20 mol%) of AlCl_3 was also dissolved in doubly distilled water and added to the polymeric solution with continuous stirring. Then the mixture solution of PVA, PVP and AlCl_3 was stirred continuously at the room temperature for several hours to obtain a homogeneous solution. The resulting solution was poured onto cleaned petri dishes and then dried in vacuum oven at 120 °C for 24 h to ensure removal of solvent traces. After drying, the films were peeled off from the petri dishes and kept in vacuum desiccators until use. X-ray diffraction (XRD) of the films was carried out using the Rigaku Miniflex-II desktop X-ray diffractometer in the range of 10–50° using $\text{CuK}\alpha$ radiation ($\lambda = 1.5406 \text{ \AA}$). The room temperature optical absorption spectra were studied using the PerkinElmer LAMBDA 35 UV–Vis–NIR spectrometer over the wavelength range of 200–800 nm. The dielectric, impedance and electric modulus measurements were performed using N4L Phase Sensitive Multimeter interfaced with Impedance Analyzer with a cell with stainless steel electrodes in the temperature range of 303–423 K over a frequency range of 100 Hz–1 MHz.

3. Results and discussion

3.1. XRD studies

Figure 1 shows the XRD patterns of AlCl_3 doped PVA–PVP films. As shown in Fig. 1(a), pure PVA–PVP film exhibits three characteristic diffraction peaks at around 14°, 17° and 20° due to the semi-crystalline nature of PVA

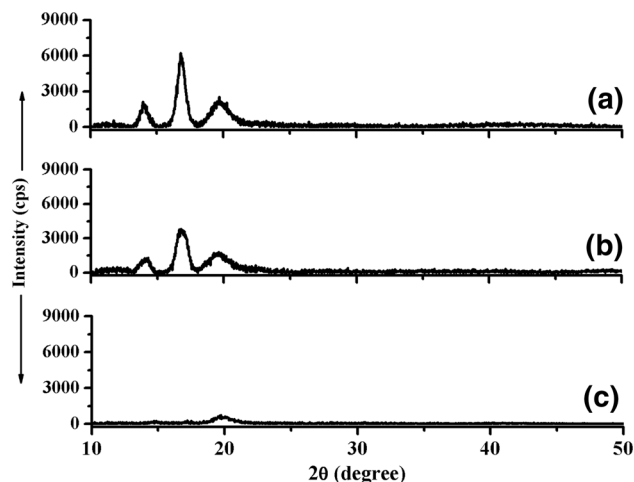


Fig. 1 XRD patterns of (a) PVA–PVP, (b) 10 mol% and (c) 20 mol% Al doped PVA–PVP polymer blend electrolyte films

[20]. No such peaks attributable to PVP could be observed. It confirms that the present polymer composite films possess both crystalline and amorphous phases. From the Fig. 1(b) and (c), it can be observed that the intensity of the peaks decreases gradually, with increase of AlCl₃ concentration, which is attributed to the interaction between the polymer composite and AlCl₃ salt. This interaction leads to decrease in intermolecular interaction between the polymer chains which causes the decrease in the degree of crystallization of PVA–PVP polymer composite films with AlCl₃ dopant concentration. Hodge et al. have been correlated a relationship between the intensity of the diffraction peaks and the degree of the crystallinity [21]. They have reported that the intensity of the XRD peaks decreases while amorphous increases with the addition of dopant concentration. For higher concentrations of AlCl₃ in the PVA–PVP blend, no sharp peaks were observed in the XRD pattern (Fig. 1(c)) which attributes the dominant role of amorphous in the complex. It also results the greater ionic diffusivity with high ionic conductivity due to amorphousness of polymers [22].

3.2. UV–Visible optical absorption studies

The UV–Visible optical absorption spectra of pure and AlCl₃ doped PVA–PVP polymer blend electrolyte films are

shown in Fig. 2(a). It is clear that the spectrum of PVA–PVP polymer blend exhibits an absorption band around 287 nm which may be attributed to π - π^* transition. It comes from unsaturated bonds (C=O and/or C=C), mainly C=O [23]. Furthermore, the optical spectra of AlCl₃ doped polymer blend films show that the absorption band position shifted towards the higher wavelength side and is found to be within the range from 293 to 298 nm as the concentration of AlCl₃ increases from 10 to 20 mol%. The absorption also increases with increase in salt concentration which implies that the increase of absorbance is approximately proportional to the AlCl₃ concentration based on the effective mass approximation. In order to determine the optical band gap of the films, the absorption coefficient (α) was determined from the following formula:

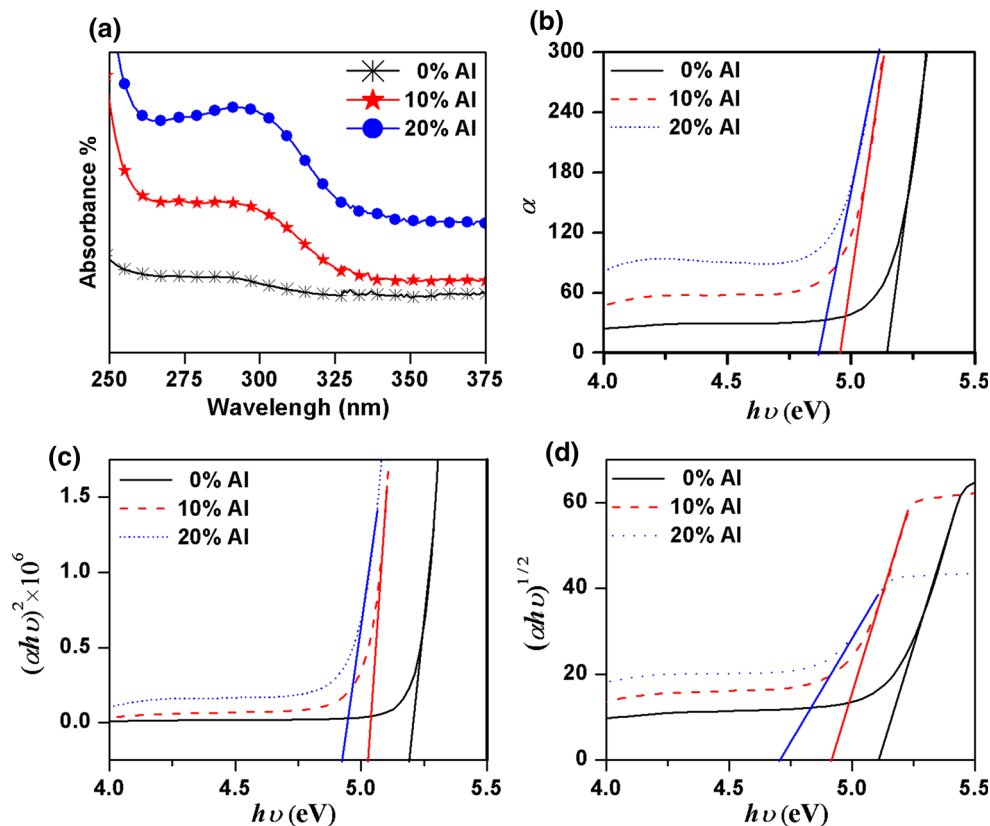
$$\alpha = 2.303 \times \frac{A}{d} \quad (1)$$

where A is the absorbance and d is the film thickness. The optical energy band gap of the films was determined from the absorption spectra near the absorption edge. The absorption coefficient dependence on photon energy is expressed as:

$$(\alpha h\nu)^r = B(h\nu - E_g) \quad (2)$$

where B is a constant, $h\nu$ is the photon energy and E_g is the optical energy band gap, r is an exponent which can take

Fig. 2 (a) Optical absorption spectra, (b) α versus $h\nu$ plots, (c) $(\alpha h\nu)^2$ versus $h\nu$ plots and (d) $(\alpha h\nu)^{1/2}$ versus $h\nu$ plots of different concentrations of Al doped PVA–PVP polymer blend electrolyte films



values of 1, 2, 3, 1/2, 3/2 depending on the nature of the electronic transitions responsible for the optical absorption [15]. The best straight line can be determined from the slope of the linear part of $(\alpha h\nu)^2$ versus $h\nu$ and $(\alpha h\nu)^{1/2}$ versus $h\nu$. This suggests that the transition energy for electrons may account for direct and indirect allowed transitions. The absorption coefficient, direct and indirect optical band gaps were estimated by extrapolating the linear portion of their curves as shown in Fig. 2(b–d). The obtained values are given in Table 1. It is clear from the Table 1 that the absorption coefficient, direct and indirect band gap values decrease with AlCl_3 doping which is due to the fact that the salt concentration significantly decreases the optical energy gap in the way of producing some defects in the polymer blend films. These defects cause the localized states which reflect the increase in the degree of disorder in films [24].

3.3. Dielectric properties

Figure 3 presents the plot of (a) real (ϵ') and (b) imaginary (ϵ'') parts of dielectric constant as a function of frequency for PVA–PVP and AlCl_3 doped PVA–PVP films. From the figure, the highest dielectric constant has been observed at lower frequencies and its value decreases with increase in frequency. It shows that the low frequency dispersions are very strong and can be associated with space charge polarization effects arising from the electrodes. In the high frequency region, due to high periodic reversal of the field at the interface, the contribution of charge carriers towards the dielectric constant decreases with increasing frequency. Hence, the dielectric constant decreases with increasing frequency [25]. It is also noticed that the dielectric constant increases with the increase in AlCl_3 dopant concentration which proves that the introduction of AlCl_3 would increase the dielectric constant of PVA–PVP film. The maximum dielectric constant at low frequency is found for 20 mol% AlCl_3 doped polymer composite film. Figure 3(c) and (d) show the dielectric plots of 20 mol% AlCl_3 doped polymer film at different temperatures. It can be seen that the dielectric constant increases with increasing temperature. This behavior is due to the fact that dipole orientation

is facilitated by increasing the temperature, thus increasing the dielectric constant. [26, 27].

3.4. Ac conductivity studies

The frequency dependent ac conductivity of various concentrations of AlCl_3 doped with PVA–PVP polymer blend electrolyte films at room temperature is shown in Fig. 4. The ac conductivity increases with increasing salt concentration, as shown in Fig. 4, which is due to an increase in the number of mobile charge carriers by the addition of AlCl_3 . Hence, it confirms that the mobility of anions has been restricted and the conductivity of polymer blend is enhanced by mobility of aluminium cations. It is also noticed that the ac conductivity of AlCl_3 doped PVA–PVP polymer blend electrolyte films is higher than that obtained in undoped PVA–PVP film. The maximum conductivity is found to be 6.89×10^{-4} S/cm at 1 MHz for 20 mol% AlCl_3 doped PVA–PVP film. The ac conductivity plots show a plateau at low frequency, which corresponds to the dc conductivity of bulk material and exhibit dispersion at high frequency, which corresponds to the ac conductivity. The conductivity increases as the frequency increases towards higher frequency side. This behavior obeys Jonchers's power law as follow:

$$\sigma_{ac}(\omega) = \sigma_0 + A\omega^n \quad (3)$$

where σ_0 is the dc conductivity of bulk material, A is the pre-exponential factor and n is the power law exponent. The values of σ_0 , A and n can be obtained by fitting the above equation and they are given in Table 1. For ideal ion conducting polymer electrolyte, n should be between 0 and 1, indicating the ideal long-range pathways and tortuous pathway. The values of n are in the range of 0.78–0.94. As given in Table 1, the increase in n with AlCl_3 doping shows that the long range drift of ions may be one of the main reasons of ionic conduction. Figure 5 represents the frequency dependent ac conductivity of 20 mol% AlCl_3 doped PVA–PVP polymer blend electrolyte film at different temperatures. The conductivity increases with increasing temperature which is common in solid polymer electrolytes. It is due to the tremendous increase of the

Table 1 Absorption edge, band gaps, σ_{ac} , σ_0 , A , n and σ_{dc} , values of PVA–PVP polymer electrolyte doped with various concentrations (x mol%) of AlCl_3 films at room temperature

x	Absorption Edge	Band gaps (eV)		$\sigma_{ac} \times 10^{-4}$ (S/cm)	$\sigma_0 \times 10^{-5}$ (S/cm)	$A \times 10^{-8}$	n	$\sigma_{dc} \times 10^{-5}$ (S/cm)
		Direct	Indirect					
0	5.14	5.19	5.10	2.88	0.0364	0.0148	0.78	0.46
10	4.95	5.02	4.91	4.20	0.1235	0.2125	0.88	2.03
20	4.89	4.92	4.70	6.89	0.9041	0.9871	0.94	8.05

Fig. 3 Dielectric plots (a) ϵ' and (b) ϵ'' of pure and Al doped PVA–PVP polymer blend electrolyte films at room temperature. (c) ϵ' and (d) ϵ'' plots of 20 mol% Al doped PVA–PVP polymer electrolyte film at different temperatures

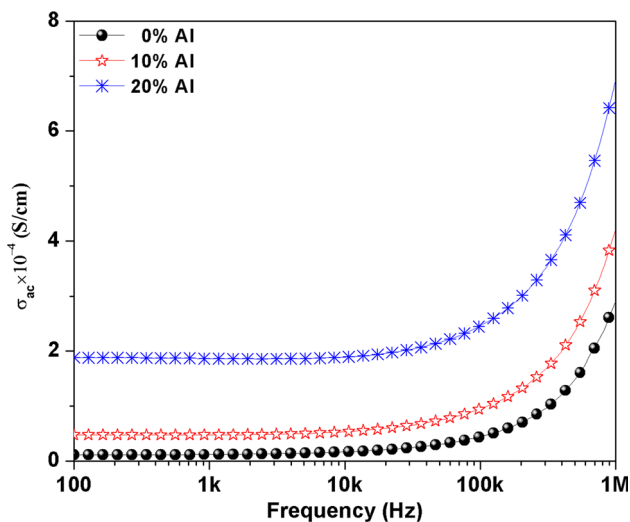
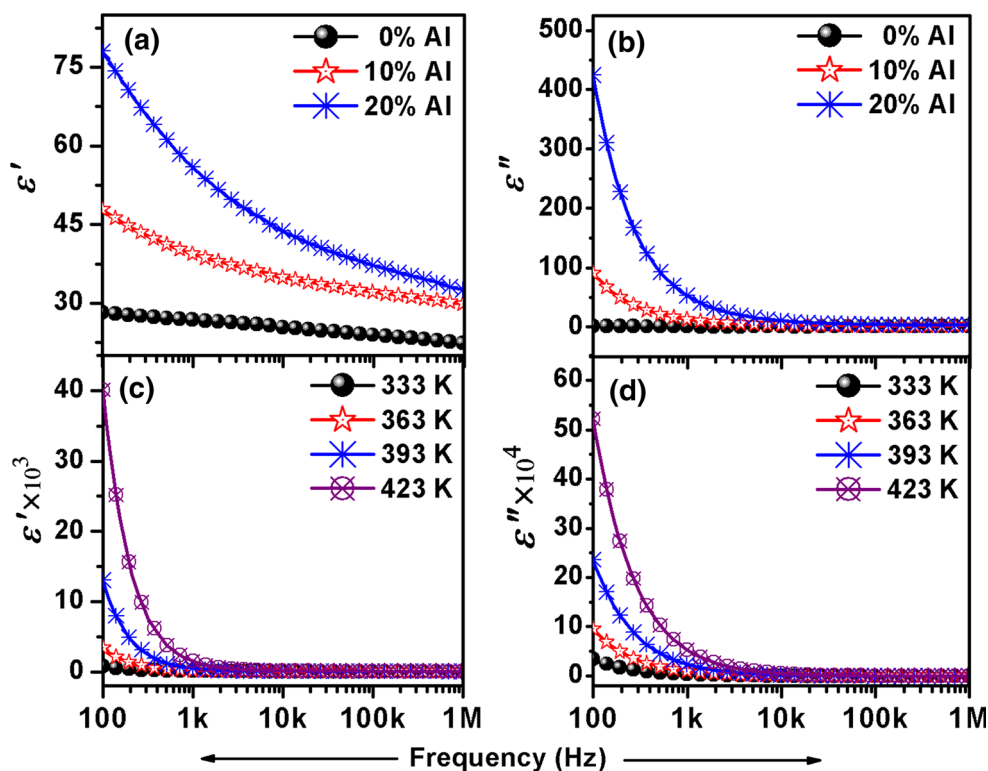


Fig. 4 ac conductivity of PVA–PVP polymer blend doped with different concentrations of AlCl₃ at room temperature

mobile charge carriers which contributes the transport of ions in polymer composite films [28].

3.5. Complex impedance analysis

The room temperature complex impedance plots of PVA–PVP and AlCl₃ doped PVA–PVP polymer blend electrolyte films are shown in Fig. 6. The plots obey the Cole–Cole type relaxation by exhibiting only one semicircular arc

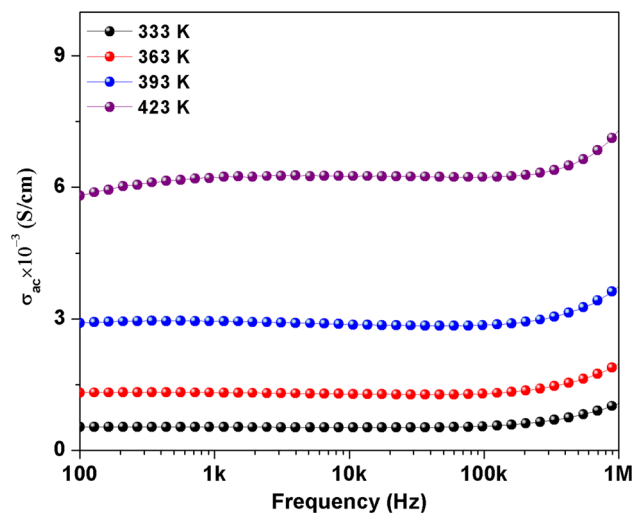


Fig. 5 ac conductivity of 20 mol% Al doped PVA–PVP polymer blend electrolyte film at different temperatures

over the entire frequency range which corresponds to the bulk properties of grain (dc resistivity). The ionic conductivity (σ_{dc}) can be calculated using the standard relation, $\sigma_{dc} = d/R_b A$, where d is the thickness of the sample, A is the area of the sample and R_b is the bulk resistance derived from the intercept of the impedance plot on real axis [15]. The ionic conductivity values of different complexes at room temperature are given in Table 1. As seen in the Table 1, the ionic conductivity increases with increase

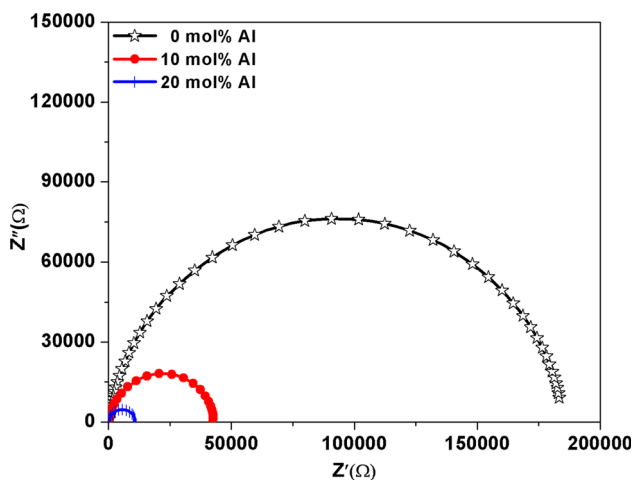


Fig. 6 Room temperature complex impedance plots of PVA-PVP and Al doped PVA-PVP polymer blend electrolyte films

in dopant concentration and found to be high for 20 mol% AlCl_3 doped film. This might be attributed to increase in number of mobile charge carriers and it results the dominant amorphous phase in the film. This would happen when the interaction between polymer and salt takes place. Also, the σ_{dc} value of 20 mol% AlCl_3 doped film is three or four orders of magnitude larger than those previously reported in certain representative metal salts doped polymer electrolytes [15, 22, 29–31]. Furthermore, the obtained value is about two orders of magnitude greater than the measured value of Li^+ -poly ethylene oxide complex [32]. Hence, it confirms that the interaction of Al^{3+} ions with polymer blend could also improve the ionic conductivity which leads them as the superior candidates against the other solid electrolytes.

Figure 7 shows the complex impedance plots of PVA/PVP/20 mol% AlCl_3 electrolyte film at different

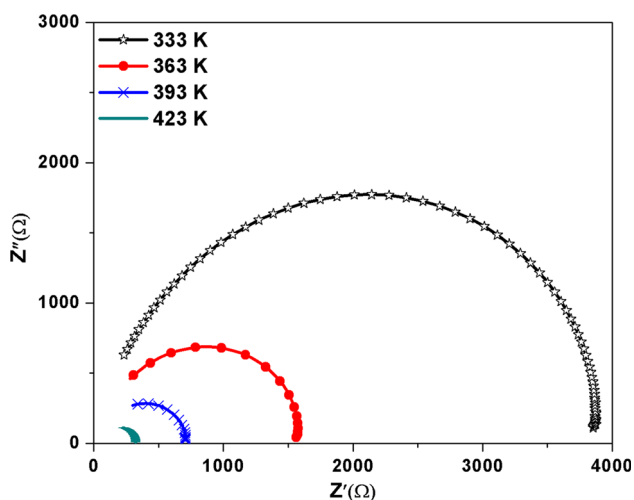


Fig. 7 Complex impedance plots of 20 mol% Al^{3+} doped PVA-PVP polymer blend electrolyte films at different temperatures

temperatures. The extrapolation of intercept of semicircular arc on the real axis tends to lower values with increasing temperature which is attributed to the enhancement in ionic conductivity. This may be explained on the basis of free volume model. When the temperature increases, the vibration energy of a segment of polymer chain becomes sufficient to push against the hydrostatic pressure imposed by its neighbouring atoms and create a small amount of space surrounding its own volume in which vibrational motion can occur. Therefore, the free volume around the polymer chain causes the mobility of the ions to increase and the segmental motion of polymer chain causes the conductivity to increase. Hence, the increase in temperature causes the conductivity to increase due to the increased free volume and segmental mobilities [33]. The plot of $\log \sigma_{dc}$ versus inverse temperature ($1000/T$) of 20 mol% AlCl_3 doped PVA-PVP film is shown in Fig. 8. The plot showed a straight line which suggests that the Arrhenius-type thermally activated process and it is represented by

$$\sigma_{dc} = \sigma_0 \exp\left(\frac{-E_a}{k_B T}\right) \quad (4)$$

where σ_0 is the pre-exponential factor, k_B is the Boltzmann constant, T is the absolute temperature and E_a is activation energy which can be calculated from the slope of the straight line fitted by the above equation to the experimental data. The activation energy is found to be 0.24 eV which is very small in comparison with E_a of other solid electrolytes. The low value of E_a is due to the amorphous nature of polymer blend that facilitates a higher free volume in the electrolyte on increasing temperature and allows Al^{3+} ions to hop from one site to another, thus increasing the conductivity.

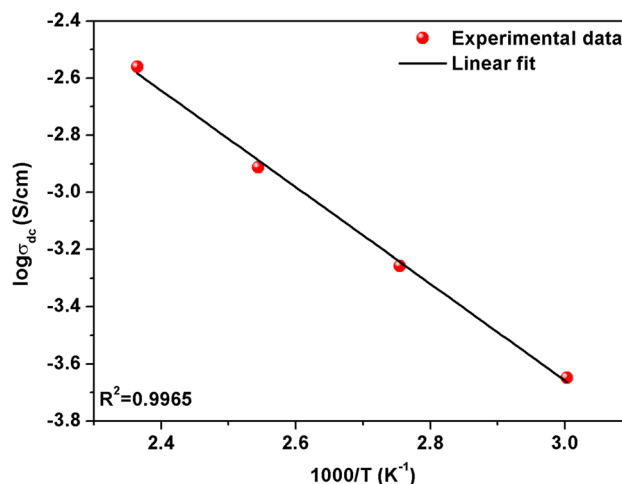


Fig. 8 Plot of $\log \sigma_{dc}$ versus $1000/T$ for 20 mol% Al doped PVA-PVP polymer electrolyte film

3.6. Electric modulus studies

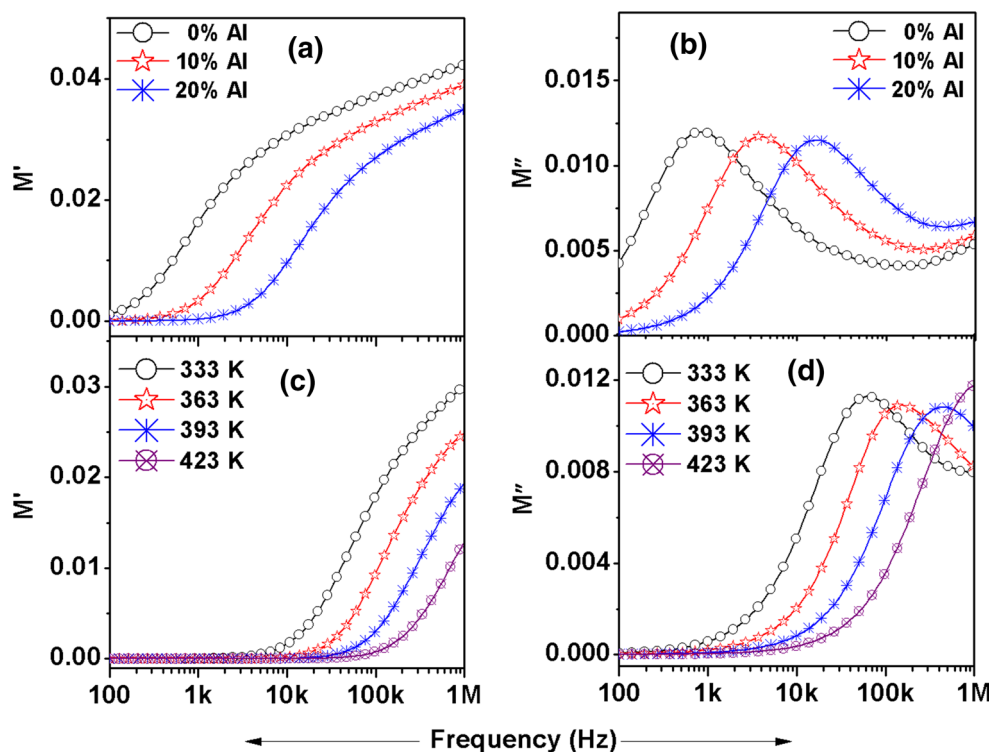
The electric modulus plots of three films are displayed in Fig. 9. In general, the dielectric materials show a plateau at lower frequencies and an abrupt increase in M' spectra at higher frequencies. The room temperature electric modulus spectra of various compositions are shown in Fig. 9(a) and (b). It can be observed from Fig. 9(a) that the values of M' for electrolyte films at low frequencies are small, which confirms the removal of electrode polarization. As shown in Fig. 9(b), the values of M'' show an asymmetric peak approximately centered in the dispersion region of M' . The peak shifts to higher frequency as the dopant concentration increases, indicating that the relaxation time decreases with increasing AlCl₃ dopant concentrations. Temperature dependent electrical modulus spectra as function of frequency for the pure and AlCl₃ doped PVA–PVP films are shown in Fig. 9(c) and (d). It is obvious from Fig. 9(c) that the asymptotic value of M' at high frequency side shows the dispersion tending towards to M_∞ due to conductivity relaxation and indicates the presence of a relaxation time. At the low frequency side, M' approaches zero, indicating that the electrode polarization gives a negligible low contribution of M' and can be ignored. In Fig. 9(d), the low value of M'' at the low frequency side might be due to the large value of capacitance associated with the electrode polarization effect, as a result of accumulation of a large amount of charge carriers at the electrode-polymer electrolyte interface. However, Fig. 9(d) shows only one peak

which is shifted towards higher frequency with increasing temperature. This might be related to thermally activated relaxation process, and charge carrier hopping takes place. The frequency region on the pre-peak decides the range whereas the mobility of charge carriers are on long distances while region to the post-peak is where the confinement of carriers in potential wells, being mobile on short distances which are consistent with conductivity studies as mentioned above [34]. The frequency maximum (f_{\max}), which corresponds to the M''_{\max} , gives the relaxation time (τ_c) from the condition, $\omega_{\max}\tau_c = 1$. The migration energy (E_m) can be calculated using the Arrhenius equation:

$$f_{\max} = f_0 \exp\left(\frac{-E_m}{kT}\right) \quad (5)$$

where f_0 is the pre-exponential factor, k is the Boltzman constant and T is the absolute temperature [15]. As shown in the Fig. 10, the E_m was estimated using least square fitting method to the experimental data and found to be 0.25 eV which is in good agreement with the E_a value obtained from the dc conductivity plot as discussed above. This result implies that the charge carriers responsible for both conductivity and relaxation are the same, and that the enthalpy of carrier formation is negligible in this system.

Fig. 9 Modulus spectra (a) M' and (b) M'' of PVA–PVP and Al doped PVA–PVP polymer blend electrolyte films. (c) M' and (d) M'' plots of 20 mol% Al doped PVA–PVP polymer electrolyte film at different temperatures



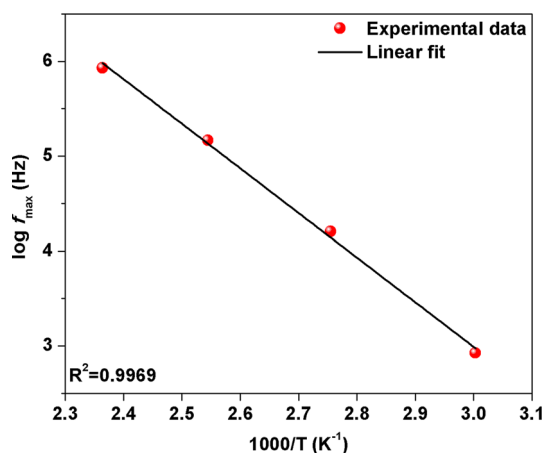


Fig. 10 Inverse temperature dependence of relaxation frequency plot of 20 mol% Al doped PVA–PVP polymer electrolyte film

4. Conclusions

Pure and AlCl_3 doped PVA–PVP polymer electrolyte films were prepared by solution casting technique. XRD patterns revealed the amorphous domains of PVA–PVP polymer blend electrolyte increased with increasing the AlCl_3 dopant. Optical absorption spectra exhibited that the values of absorption edge, direct and indirect band gaps are decreased with increase in salt concentration. This result indicates the formation of charge transfer complexes between polymer and AlCl_3 dopant. The plots of dielectric constant showed an increase in the dielectric constant at low frequency with AlCl_3 concentration and are attributed to the presence of space charge polarization phenomena at the electrodes. Frequency dependent ac conductivity of films obeys Jonscher power law and its value found to be increase with increasing dopant concentration. From the complex impedance plots, the ionic conductivity was calculated and is higher for 20 mol% AlCl_3 doped PVA–PVP polymer electrolyte film. The obtained room temperature ionic conductivity value is three or four orders of magnitude larger than those previously reported on certain representative polymer-salt complexes. Temperature dependence of ionic conductivity showed a single semicircular arc over the temperature range of 323–403 K while the two semicircular arcs appeared at above 403 K temperature. The removal of electrode polarization was confirmed by the electrical modulus plots which exhibits the decrease in conductivity relaxation time with Al doping. The migration energy was estimated from the temperature dependent electric modulus plot and is found to be 0.25 eV. This value is agreed well with the activation energy estimated from the temperature dependent dc conductivity plot. The electrical conduction of the sample was depicted using an equivalent circuit. These results suggest

that the AlCl_3 doped PVA–PVP electrolyte films are potential candidate for electrochemical device applications.

Acknowledgements The authors gratefully acknowledge the financial support from University Grants Commission (UGC), New Delhi, India, to undertake this work (Grant No. F.39-494/2010 (SR)).

References

- [1] M B Armond *Ann. Rev. Mater. Sci.* **16** 245 (1986)
- [2] M A Ratner and D F Shriver *Chem. Rev.* **88** 109 (1988)
- [3] M Watanabe, K Sanui, N Ogata, F Inoue, T Kobayashi and Z Ohtaki *Polym. J.* **16** 711 (1984)
- [4] L Lee, S Park and S Kim *Solid State Ionics* **234** 19 (2013)
- [5] M C Wintergrill, J J Fontanella, M K Smith, S S Greenbaum, K J Adam and C C Andeen *Polymer* **28** 633 (1987)
- [6] J Prochanski, W Wicxorek, J Przyłuski and K Such *Appl. Phys. A.* **49** 55 (1989)
- [7] N Reddeppa, T J R Reddy, V B S Achari, V V R N Rao and A K Sharma *Ionics* **15** 255 (2009)
- [8] Y H Liang, C.Y. Hung and C C Wang *J. Power Sour.* **188** 261 (2009)
- [9] R Baskaran, S Selvasekarapandian, N Kuwata, J Kawamura and T Hattori *Mater. Chem. Phys.* **98** 55 (2006)
- [10] N F Mott and E A Davis *Electronic Processes in Non-crystalline Materials*, 2nd edn. (Oxford: Clarendon Press) W H Marshall and D H Wilkinson 270 (1972)
- [11] S Ramesh and O L Ling *Polym. Chem.* **1** 702 (2010)
- [12] B Natesan, N K Karan and R S Katiyar *Phys. Rev. E.* **74** 042801 (2006)
- [13] H M Ragab *Physica B.* **406** 3759 (2011)
- [14] M Hema, S Selvasekerapandian, A Sakunthala, D Arunkumar and H Nithya *Physica B.* **403** 2740 (2008)
- [15] V Krishnakumar and G Shanmugam *Ionics* **18** 403 (2012)
- [16] K Kiran Kumar, M Ravi, Y Pavani, S Bhavani, A K Sharma and V V R Narasimha Rao *Phys. B.* **406** 1706 (2011)
- [17] M A F Basha *Polym. J.* **42** 728 (2010)
- [18] N Imanaka, Y Hasegawa, M Yamaguchi, M Itaya, S Tamura and G Adachi *Chem. Mater.* **14** 4481 (2002)
- [19] L Zhang, P Chen, Z Hu and C Chen-hua *Chin. J. Chem. Phys.* **25** 703 (2012)
- [20] G K Prajapati and P N Gupta *Physica B.* **406** 3108 (2011)
- [21] R M Hodge, G H Edwrđ and E P Simon *Polymer.* **37** 1371 (1996)
- [22] A A Mohamad, N S Mohamad, M Z A Yahya, R Othman, S Ramesh, Y Alias and A K Aroof *Solid State Ionics.* **156** 171 (2003)
- [23] E M Abdelrazek *Physica B.* **403** 2137 (2008)
- [24] Y Aydogdu, F Yakuphanoglu, A Aydodu, E Tas and A Cukuraval *Solid State Sci.* **4** 879 (2002)
- [25] J R MacCullum and C R Vincent *Polymer Electrolytes Reviews-2* (England: Elsevier Science Publishers Ltd) (1989)
- [26] A Awadhia, S K Patel and S L Agrawal *Prog. Cryst. Growth Charact. Mater.* **52** 61 (2006)
- [27] X Sun, T Fujimoto and H Uyama *Polym. J.* **45** 1101 (2013)
- [28] P Sharma and D K Kanchan *Polym. Int.* **63** 290 (2014)
- [29] M Watanabe, S Nagona, K Sanui and N Ogata *J. Power Sour.* **20** 327 (1987)
- [30] D K Pradhan, R N P Choudhary and B K Samantaray *Express Polym. Lett.* **2** 630 (2008)
- [31] V Krishnakumar and G Shanmugam *Sci. Adv. Mater.* **4** 1247 (2012)
- [32] S- W Ryu *Polym. J.* **40** 688 (2008)

[33] G Hirankumar, S Selvasekarapandian, M S Bhuvaneswari, R Baskaran and M Vijayakumar *J. Solid State Electrochem.* **10** 193 (2006)

[34] S B Aziz, Z H Z Abidin and A K Arof *Express Polym. Lett.* **4** 300 (2010)